

CHEMISTRY OF MATERIALS

VOLUME 15, NUMBER 19

SEPTEMBER 23, 2003

© Copyright 2003 by the American Chemical Society

Communications

Synthesis of Highly Coherent SiGe and Si₄Ge Nanostructures by Molecular Beam Epitaxy of H₃SiGeH₃ and Ge(SiH₃)₄

Changwu Hu,[†] Jennifer L. Taraci,[‡] John Tolle,[‡]
Matthew R. Bauer,[‡] Peter A. Crozier,[§]
Ignatius S. T. Tsong,[†] and John Kouvetakis^{*‡}

*Department of Physics and Astronomy, Department of
Chemistry and Biochemistry, and Center for
Solid State Science, Arizona State University,
Tempe, Arizona 85287*

Received June 12, 2003

Revised Manuscript Received July 5, 2003

The growth of Si_{1-x}Ge_x films on Si(100) has been the subject of intensive studies over the past 2 decades owing to their many important applications in high-speed microelectronic devices.¹⁻⁴ A number of different methods have been used for the heteroepitaxial growth of Si_{1-x}Ge_x/Si, but the two most commonly employed techniques are molecular beam epitaxy (MBE) utilizing solid Si and Ge and ultrahigh vacuum chemical vapor deposition (UHV-CVD) or gas-source molecular beam epitaxy (GSMBE) utilizing SiH₄ and GeH₄ or Si₂H₆ and Ge₂H₆. There are two ultimate, but also diverse, objectives in the growth of Si_{1-x}Ge_x/Si. The first is the achievement of defect-free Si_{1-x}Ge_x layers, which may take the form of strained layer superlattices, while the

second is the growth of self-assembled coherent Si_{1-x}Ge_x islands or quantum dots.

Here, we describe for the first time a unique approach to grow Si_{1-x}Ge_x films and nanometer-scale islands by using single-source molecular hydrides containing direct Si-Ge bonds. The growth process effectively occurs via single-source GSMBE. The composition *x* of the film is predetermined by tailoring the composition of the molecular precursor. We demonstrate our technique by growing Si_{0.5}Ge_{0.5} and Si_{0.8}Ge_{0.2} epitaxial films and coherent islands on Si(100) via thermal dehydrogenation of H₃SiGeH₃ and Ge(SiH₃)₄,⁵ respectively, between 475 and 700 °C. The major advantages of using a single molecular source for the MBE growth of Si_{1-x}Ge_x lie not only in the a priori control over the composition but also in the ability of the film morphology to be controlled by the adjustment of a single kinetic parameter, that is, the flux rate of the precursor, at a given temperature.

The growth of the Si_{0.5}Ge_{0.5} and Si_{0.8}Ge_{0.2} films on Si(100) was conducted in the sample chamber of a low-energy electron microscope (LEEM) where in situ observation of the growth process took place in real time. The base pressure of the LEEM chamber was 2 × 10⁻¹⁰ Torr. Film growth was accomplished using partial pressures of about 10⁻⁶ Torr. Figure 1 shows a sequence of frame-captured LEEM video images over a field of view of 8 μm of Si_{0.5}Ge_{0.5} growth on Si(100)-(2 × 1) at 550 °C. The LEEM images were taken with the (1/2,0) diffraction beam such that the (2 × 1) and (1 × 2) terraces separated by single-height atomic steps alternate in contrast from dark to bright due to the rotation of the dimer reconstruction across a step. The last LEEM frame taken at 46 min showing island formation was a bright-field image acquired using the (0,0) beam. In Figure 1, contrast reversal in the (2 × 1) and (1 × 2)

* To whom correspondence should be addressed.

[†] Department of Physics and Astronomy.

[‡] Department of Chemistry and Biochemistry.

[§] Center for Solid State Science.

(1) Patton, G. L.; Harnage, D. L.; Stroock, J. M.; Meyerson, B. S.; Scilla, G. S. *IEEE Electron Device Lett.* **1989**, 10, 534.

(2) Mooney, P. M.; Chu, J. O. *Annu. Rev. Mater. Sci.* **2000**, 30, 335.

(3) Tromp R. M.; Ross, F. M. *Annu. Rev. Mater. Sci.* **2000**, 30, 431.

(4) Brunner, K. *Rep. Prog. Phys.* **2002**, 65, 27.

(5) Lobreyer, T.; Oberhammer, H.; Sudenmeyer, W. *Angew. Chem., Int. Ed. Engl.* **1993**, 32, 586.

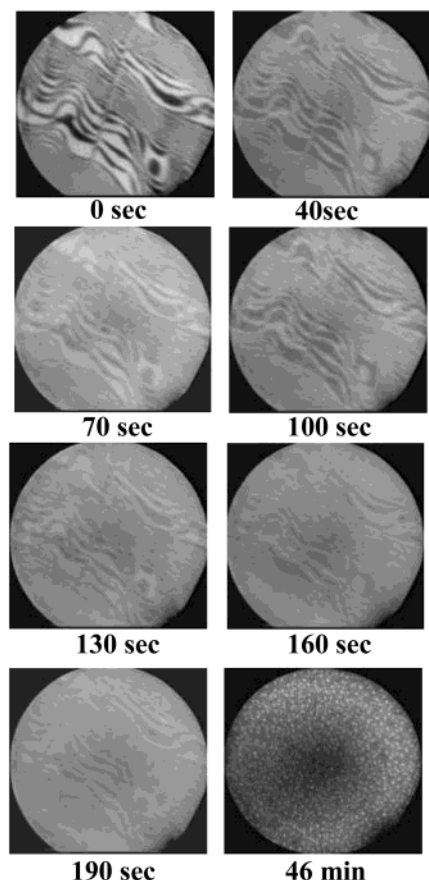


Figure 1. Frame-captured LEEM video images showing Stranski-Krastanov growth of $\text{Si}_{0.5}\text{Ge}_{0.5}$ at 570°C . The elapsed time during growth is indicated under each frame. Approximate Si-Ge coverage for each frame: 0 ML at 0 s; 1 ML at 40 s; 2 ML at 70 s; 3 ML at 100 s; 4 ML at 130 s; 5 ML at 160 s; 6 ML at 190 s; and 3D islands at 46 min. Field of view is $8\ \mu\text{m}$.

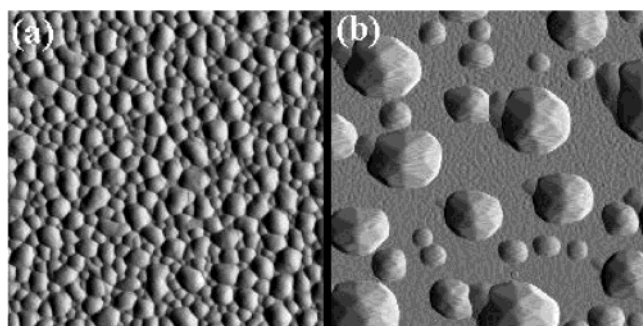


Figure 2. AFM images of 3D $\text{Si}_{0.5}\text{Ge}_{0.5}$ islands grown at (a) 570°C and (b) 700°C . Scan area is $2 \times 2\ \mu\text{m}^2$.

terraces was observed during the time lapse from 0 to 190 s as growth of $\text{Si}_{0.5}\text{Ge}_{0.5}$ proceeded. Such contrast reversal on the $\text{Si}(100)-(2 \times 1)$ surface is indicative of layer-by-layer growth.⁶ With the exception of the first contrast reversal, which took 40 s, each subsequent complete reversal took place in a time interval of 30 s. This means that the growth of a full $\text{Si}_{0.5}\text{Ge}_{0.5}$ monolayer (ML) is completed every 30 s. We found from our LEEM observations that the first ML consistently took a little longer to complete, for example, 40 s in the first frame of Figure 1, than the subsequent layers. The layer-by-

layer growth continued up to 190 s, after the completion of 6 ML, after which the LEEM contrast of the surface became very diffuse. The loss of contrast was probably due to new layers growing on top of incomplete layers as reported in scanning tunneling microscopy (STM) observations.⁷ This kind of growth results in a rough surface, even though the domains are two-dimensional (2D), contributing to the loss of LEEM contrast. Three-dimensional (3D) islands began to appear after about 18 min of growth. The last frame shown in Figure 1 is a bright-field LEEM image taken after 46 min of growth with the 3D islands appearing as bright spots. Since our LEEM has a lateral resolution of $\sim 10\ \text{nm}$, it is not known exactly at what growth time that the 3D islands started to nucleate. Although we could not pinpoint the transition from 2D to 3D growth, our LEEM results nevertheless suggest that the growth mode of the $\text{Si}_{0.5}\text{Ge}_{0.5}$ is Stranski-Krastanov.

The morphology and size of the $\text{Si}_{0.5}\text{Ge}_{0.5}$ islands were further examined ex situ by atomic force microscopy (AFM) and cross-sectional transmission electron microscopy (XTEM). The AFM images of $\text{Si}_{0.5}\text{Ge}_{0.5}$ islands grown at 570°C and 700°C are presented in Figure 2. These are primarily large dome-shaped islands associated with later stages of growth. The island densities, however, are quite different for the two growth temperatures. The islands grown at 570°C in Figure 2a are reasonably uniform in size, with a density of $\sim 6 \times 10^9\ \text{cm}^{-2}$. The islands grown at 700°C show a bimodal distribution, with the smaller ca. 100-nm-wide islands having a density of $\sim 5 \times 10^8\ \text{cm}^{-2}$ and the larger ca. 400-nm-wide islands having a density of $\sim 2.5 \times 10^8\ \text{cm}^{-2}$. The high density at 570°C in Figure 2a is confirmed by XTEM studies, which show the presence of isolated, closely spaced, and uniform in size islands. The lower island density at 700°C is probably the result of a longer diffusion length of the Si/Ge species at the higher growth temperature. The bimodal distribution of island sizes (at 700°C) could be a result of unsaturated Ostwald ripening, which operates at longer diffusion lengths or some other more complex coarsening mechanisms.⁸ At the lower 570°C growth temperature, the lower mobility of the Si/Ge species results in denser nucleation sites and therefore a higher island density. The dome shape of these islands with $\{113\}$ and $\{15\ 3\ 23\}$ facets³ is clearly demonstrated in the XTEM image Figure 3 (a) of an island grown at 570°C . The island, 60 nm in width, is completely coherent. We have also observed by XTEM 110-nm-wide islands grown at 700°C that are also completely coherent, demonstrating the fact that our single source approach is capable of producing large coherently strained dome-shaped islands. Finally, it is interesting to note that deposition of H_3SiGeH_3 at extremely low temperatures ($450\text{--}470^\circ\text{C}$) resulted in growth of highly coherent $\text{Ge}_{0.50}\text{Si}_{0.50}$ quantum dots that were fairly uniform in size (10–15-nm width, 3–5-nm height) shape and spatial distribution as illustrated in Figure 3 (b).

Growth of $\text{Si}_{0.8}\text{Ge}_{0.2}$ films on $\text{Si}(100)$ was conducted using the $\text{Ge}(\text{SiH}_3)_4$ gaseous source at 500, 600, and

(7) Voigtländer, B. *Surf. Sci. Rep.* **2001**, *43*, 127.

(8) Ross, F. M.; Tersoff, J.; Tromp, R. M. *Phys. Rev. Lett.* **1998**, *80*, 984.

(6) Tromp R. M.; Reuter, M. C. *Phys. Rev. Lett.* **1992**, *68*, 954.

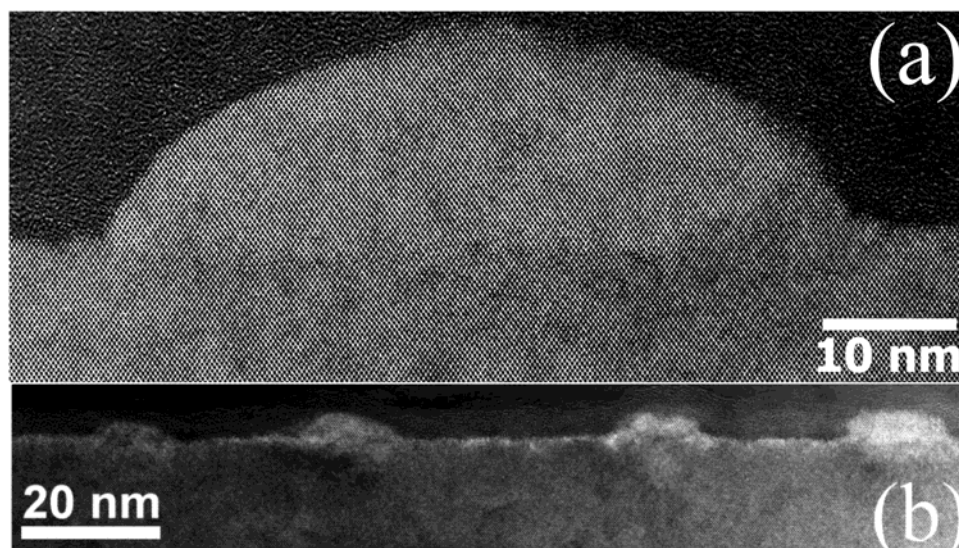


Figure 3. High-resolution XTEM image of perfectly coherent $\text{Si}_{0.5}\text{Ge}_{0.5}$ nanostructures: (a) a dome-shaped island grown at 570 °C; (b) a periodic array of quantum dots with uniform size distribution grown at 470 °C.

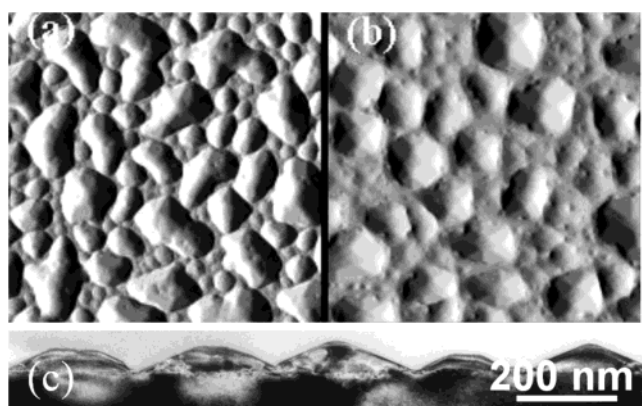


Figure 4. AFM images of 3D $\text{Si}_{0.8}\text{Ge}_{0.2}$ islands grown at (a) 500 and (b) 700 °C. Scan area is $2 \times 2 \mu\text{m}^2$. (c) XTEM dark field image of periodic arrays of $\text{Si}_{0.8}\text{Ge}_{0.2}$ islands grown at 600 °C.

700 °C. In situ real-time LEEM observations of the growth were similar to that shown in Figure 1; that is, the Stranski-Krastanov growth mode was in operation. The 3D island formation through nucleationless strain-driven morphological instability^{9,10} was not observed in any of the LEEM growth sequences of $\text{Si}_{0.5}\text{Ge}_{0.5}$ and $\text{Si}_{0.8}\text{Ge}_{0.2}$ using our single-source MBE approach. Figure 4 shows AFM images of the surface morphology of films grown at 500 and 700 °C after a growth period of 60 min. Large faceted dome-shaped islands are observed at this late stage of growth at both temperatures, but the islands grown at the lower temperature (500 °C) appear more irregular than those grown at 700 °C. This is attributed to the enhanced mobility of the diffusing species at higher growth temperatures, resulting in the more symmetrical shapes. High-resolution XTEM images of the large islands of widths between 200 and 400 nm show that they are dislocated domes (Figure 4c). Selected area electron diffraction patterns of these relaxed islands show a lattice constant of $5.48 \pm 0.01 \text{ \AA}$, very close to the ideal 5.476 \AA for $\text{Si}_{0.8}\text{Ge}_{0.2}$.

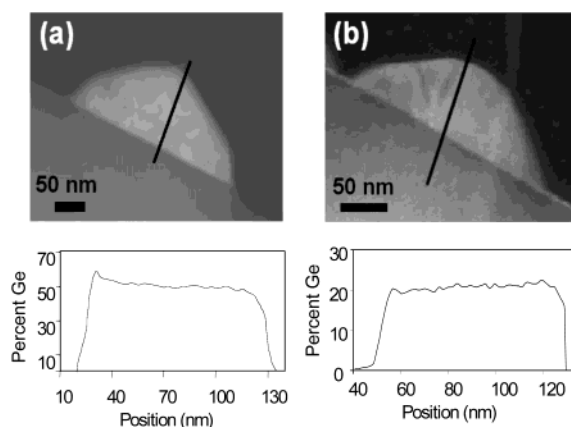


Figure 5. Ge composition line scans determined by high-resolution EELS on (a) a $\text{Si}_{0.5}\text{Ge}_{0.5}$ island grown at 700 °C and (b) a $\text{Si}_{0.8}\text{Ge}_{0.2}$ island grown at 500 °C. The profiles shown below each XTEM image correspond to the line across the substrate/island interface. Scan direction is from the substrate to the vacuum.

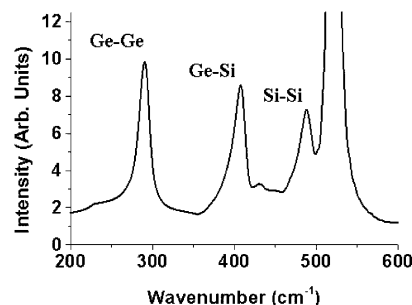


Figure 6. Raman spectrum of a $\text{Si}_{0.50}\text{Ge}_{0.50}$ film showing the Si-Si, Si-Ge, and Ge-Ge peaks of the film and the Si peak of the substrate (off scale).

We conducted high spatial resolution electron energy loss spectroscopy (EELS) and Raman spectroscopy to verify that the composition of the $\text{Si}_{1-x}\text{Ge}_x$ materials indeed reflects the stoichiometry of the precursor used for growth. Typical EELS composition line scans across the interface from the substrate to the island using an electron beam with 1-nm diameter are given in Figure 5. The composition profile of a $\text{Si}_{0.5}\text{Ge}_{0.5}$ island grown

(9) Sutter P.; Lagally, M. G. *Phys. Rev. Lett.* **2000**, *84*, 4637.

(10) Tromp, R. M.; Ross, F. M.; Reuter, M. C. *Phys. Rev. Lett.* **2000**, *84*, 4641.

at 700 °C in Figure 5a shows an almost constant 50% Ge within the island. Similarly, the composition profile of a $\text{Si}_{0.8}\text{Ge}_{0.2}$ island in Figure 5b shows a nearly constant 20% Ge. No segregation of Ge is observed in any of our EELS profiles of the islands, in contrast to the report of Walther et al.,¹¹ whose EELS measurements showed vertical Ge segregation along the growth direction in 30-nm-thick $\text{Si}_{0.8}\text{Ge}_{0.2}$ layers. To characterize the local bonding environment of the Si–Ge nanostructures, the Raman spectra of each sample were recorded. Figure 6 shows the Raman spectrum of a $\text{Si}_{0.50}\text{Ge}_{0.50}$ sample and is reminiscent of those of $\text{Si}_x\text{Ge}_{1-x}$ alloys, with three main features that are known in the literature as the “Ge–Ge”, “Si–Ge”, and “Si–Si” peaks. With use of the Raman shifts associated with these peaks, the Ge compositions for selected samples were determined to be close to the values obtained by EELS.¹²

(11) Walther, T.; Humpreys, C. J.; Cullis, C. J. *Appl. Phys. Lett.* **1997**, 71, 809.

The control of composition x of $\text{Si}_{1-x}\text{Ge}_x$ films at the atomic level is achieved via the design of single-source precursors containing precise atomic arrangements with direct Si–Ge bonds. Uniform composition reflecting the stoichiometry of the precursor is observed in all cases without any segregation of either Ge or Si. The growth of $\text{Si}_{1-x}\text{Ge}_x$ films proceeds via the Stranski-Krastanov growth mode. Morphological control of the size and shape of the islands is achieved by simple adjustments of the precursor flux rate and the growth temperature.

Acknowledgment. This work was supported by the NSF grants DMR-0221993 and DMR-0303237 and the Army Research Office DAAD19-00-1-0471.

CM034477W

(12) Menéndez, J. In *Raman Scattering in Materials Science*; Weber, W. H., Merlin, R., Eds.; Springer: Berlin, 2000; Vol. 42, p 55.